Third-harmonic generation for the study of *Caenorhabditis elegans* embryogenesis

Rodrigo Aviles-Espinosa
Susana I. C. O. Santos
Institut de Ciències Fotòniques, The Institute of Photonic Sciences
Mediterranean Technology Park
Av. Canal Olimpic s/n
08860 Castelldefels, Barcelona
Spain

Andreas Brodschelm
Wilhelm G. Kaenders
TOPTICA Photonics AG
Lochhamer Schlag 19
D-82166 Graefelfing, Germany

Cesar Alonso-Ortega
Institut de Ciències Fotòniques, The Institute of Photonic Sciences
Mediterranean Technology Park
Av. Canal Olimpic s/n
08860 Castelldefels, Barcelona
Spain

David Artigas
Institut de Ciències Fotòniques, The Institute of Photonic Sciences
Mediterranean Technology Park
Av. Canal Olimpic s/n
08860 Castelldefels, Barcelona
Spain
and
Universitat Politècnica de Catalunya
Department of Signal Theory and Communications
c/Jordi Girona 31
08034 Barcelona
Spain

Pablo Loza-Alvarez
Institut de Ciències Fotòniques, The Institute of Photonic Sciences
Mediterranean Technology Park
Av. Canal Olimpic s/n
08860 Castelldefels, Barcelona
Spain

Abstract. Live microscopy techniques (i.e., differential interference contrast, confocal microscopy, etc.) have enabled the understanding of the mechanisms involved in cells and tissue formation. In long-term studies, special care must be taken in order to avoid sample damage, restricting the applicability of the different microscopy techniques. We demonstrate the potential of using third-harmonic generation (THG) microscopy for morphogenesis/embryogenesis studies in living *Caenorhabditis elegans* (*C. elegans*). Moreover, we show that the THG signal is obtained in all the embryo development stages, showing different tissue/structure information. For this research, we employ a 1550-nm femtosecond fiber laser and demonstrate that the expected water absorption at this wavelength does not severely compromise sample viability. Additionally, this has the important advantage that the THG signal is emitted at visible wavelengths (516 nm). Therefore, standard collection optics and detectors operating near maximum efficiency enable an optimal signal reconstruction. All this, to the best of our knowledge, demonstrates for the first time the noninvasiveness and strong potential of this particular wavelength to be used for high-resolution four-dimensional imaging of embryogenesis using unstained *C. elegans in vivo* samples. [DOI: 10.1117/1.3477535]

Keywords: multiphoton processes; nonlinear microscopy; fiber laser; biological imaging; functional monitoring and imaging; three-dimensional microscopy; time-resolved imaging.

Paper 10128RR received Mar. 15, 2010; revised manuscript received Jun. 9, 2010; accepted for publication Jun. 23, 2010; published online Aug. 6, 2010.

1 Introduction

Live microscopic recordings have enabled researchers to understand the developing mechanisms involved in cells and tissue formation. One particular case is the study of embryogenesis using the soil nematode *Caenorhabditis elegans* (*C. elegans*). This has been addressed employing different microscopy techniques. To perform these recordings, for example, a combination of differential interference contrast (DIC)/Nomarski and fluorescence microscopy[1–6] has been used to track morphogenesis processes *in vivo*. DIC microscopy uses polarized light allowing it to capture intrinsic features of thin transparent specimens (preferentially). This produces a contrast that is generated from the encoded phases inside the sample, but it lacks being specific to structures, and it possesses limited axial resolution.[7,8] If the development of a specific structure needs to be recorded individually, other techniques, such as fluorescence microscopy, have to be

Address all correspondence to Pablo Loza-Alvarez, ICFO—The Institute of Photonic Sciences, Mediterranean Technology Park, Av. Canal Olimpic s/n, 08860 Castelldefels, Barcelona, Spain. Tel: 34-9-3553-4075; Fax; 34-9-3553-4000; E-mail: pablo.loza@icfo.es

1083-3668/2010/15(4)/046020/7/$25.00 © 2010 SPIE

used.[9] In such a case, the use of fluorescent markers or vital dyes endogenously expressed is required for a selective observation. This has, however, time, technical, and sample viability limitations besides the inability to produce high-resolution three-dimensional (3-D) images.[10]

Given this, alternative research works have proposed the use of confocal laser scanning microscopy to compare wild-type organisms, studying a large number of existent mutant alleles and transgenic reporter strains. All this has been used to perform lineage analysis and recordings of embryogenesis in *C. elegans*.[11]

However, this technique requires the use of fluorescent reporters. Moreover, as the technique is based on linear excitation, care should be taken to minimize photodamage effects (i.e., photobleaching and phototoxicity). In addition, the excitation power must be dynamically adjusted to allow for long-term recordings in order to reduce exposure effects on the sample.[11] As a consequence, the dim signal of the system can limit the cell identification task. Therefore, to track cells and morphological processes, the development of relatively complex algorithms[12] or specialized cell tracking software is required (i.e., Endrov[2] and Simi-Biocell[4]).

A successful implementation using two-photon excited fluorescence (TPEF) to perform four-dimensional (4-D) developmental analyses in *C. elegans* was reported by in Ref. 13. Due to the reduced sample damage (based on the nonlinear effect using excitation wavelengths in the near infrared), it is possible to image living specimens for long periods. However, the use of fluorescent probes is still required.

Alternative methods, such as second-harmonic generation (SHG), and third-harmonic generation (THG), offer the advantage of being label-free techniques. These valuable tools have been used to study *in vivo* biological samples (i.e., *C. elegans, Drosophila melanogaster,* and Zebrafish).[14–22] For instance, these studies aim to establish higher harmonic imaging modalities as label-free techniques showing a great potential to perform different developmental studies in a less invasive way. The generation of SHG signal requires a noncentrosymmetric structure, limiting its applicability in tissue mainly to collagen, muscle, and microtubules.[23] In contrast, for the case of THG, the only imposition to generate a signal is the existence of interfaces (change in the refractive index or in the χ^3 nonlinear coefficient).[24] Additionally, a significant THG signal has been reported to arise from lipid bodies in different samples such as *Drosophila melanogaster*, fresh mouse lung tissue, *Arabidopsis thaliana*, etc.[19,21,25,26]

In particular, in the past, the use of wavelengths within the range of the 1500 nm from a synchronously pumped optical parametric oscillator (OPO) has been reported. In these experiments, fixed samples such as neurons and epithelial cells have been imaged using the THG technique.[27] Recently, the development of fiber-based femtosecond lasers has simplified the integration of nonlinear microscopy (NLM) techniques in biology, due to the compact design, output wavelength, pulse duration, and repetition rates of these new generation sources.[24] These lasers use reliable state-of-the-art telecommunications components that have been developed for long-term operation, minimum maintenance, and moderate cost. Thus, a fiber laser operating at 1560 nm has been used, e.g., to produce THG images of chloroplasts and flowing erythrocytes.[24]

In this work, we show the potential of the THG technique to be used for time-lapse studies in developmental processes. This is done by using a fiber-based mode-locked femtosecond telecommunications laser operating at 1550 nm. We show that employing this wavelength, it is possible to produce THG images of embryogenesis/morphogenesis process *in vivo* in *C. elegans* embryos in a noninvasive (label-free) way. The use of this specific wavelength has the advantage that the emitted THG signal is located at the visible range of the spectrum (516 nm). As a result, the requirement of UV-grade optics is eliminated, and therefore, standard photo multiplier tubes (PMTs) can be used, as they have a maximum detection efficiency located within the visible range. This wavelength has not been used in living samples or for long-term exposure experiments, and therefore, the sample viability is unknown. On one hand, UV light is not involved in the imaging process, increasing the sample viability. On the other hand, water absorption caused by the excitation wavelength starts to be important. For this reason, in this work, and in addition to the demonstration of THG microscopy at $\lambda = 1550$ nm, we confirm that it is possible to perform 4-D (time-lapse 3-D) studies for several hours in living organisms.

The emitted THG signal was present in all the developmental stages of the embryo, enabling the identification of tissues/structures and showing its potential for embryogenesis/morphogenesis studies. As a result, to the best of our knowledge, this is the first time that THG imaging at this wavelength is used to obtain 4-D embryogenesis/morphogenesis information of *C. elegans in vivo* samples.

2 Materials and Methods

2.1 *Experimental Setup*

The experimental setup was based on an inverted microscope (Nikon, Eclipse TE 2000U) modified to work as a laser scanning THG microscope.

A compact fiber-based pulsed laser system (Toptica Photonics, FemtoFiber FFS laser) operated at a central wavelength of 1550 nm, having a pulse duration of 100 fs and repetition rate of 107 MHz, was employed to excite the sample. The laser delivered an output average power up to 350 mW. An RG1000 filter (Schott; transmittance: 830 to 2000 nm) was placed at the laser output to block any spurious signal below 1000 nm from the laser itself. After passing through all the optical elements (see Fig. 1), the measured average power was 4.9 mW (measured at the sample plane), which corresponds to 460-W peak power.

The microscope is equipped with a pair of *x-y* galvanometric mirrors (GMs) (Cambridge Technology, 6215H) used to scan the excitation beam over the sample at the maximum scanning speed of ~300 lines/s. A filter cube, containing a silver-coated mirror to direct the excitation beam toward the sample, was used. A 40× oil immersion microscope objective with NA=1.3 (Nikon, Plan Fluor) was used during the experiments. The THG signal was collected by an oil immersion condenser, NA=1.4 (Nikon). A custom-made forward-detection mount using an attached photomultiplier tube (PMT; Hamamatsu, H9305-04) to detect the THG signal at the central wavelength of 516 nm was implemented. (No requirement on specialized collection optics are imposed.) This

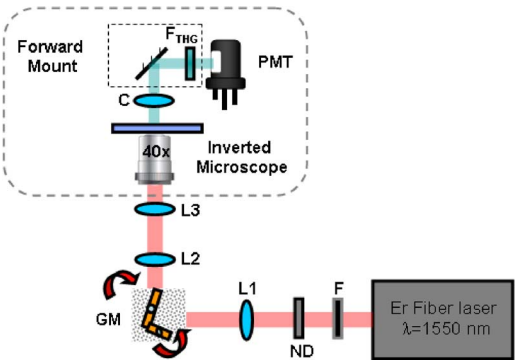

Fig. 1 Schematic of the experimental setup used for third-harmonic generation (THG). Er Fiber laser is the FemtoFiber FFS laser at 1550 nm; F, RG1000 bandpass filter; ND, neutral density filters; Li, lenses; GM, galvanometric mirrors; C, condenser (NA=1.4); F_{THG}, bandpass filters (transmittance=512–521 nm); and PMT, photomultiplier tube.

mount contained a bandpass filter to separate the fundamental beam from the generated THG signal (Semrock; transmittance: 512 to 521 nm). A homemade LabView interface was used to control both scanning units and the data acquisition card.

2.2 *Biological Sample*

Wild-type (N2) *C. elegans* embryo samples were used to perform the THG 4-D recordings. This nematode was selected because it is a widely used model organism for many different research fields. Its short life cycle, small size, transparency, invariant cell lineage, and ease of maintenance in the lab make this model organism highly attractive for microscopy studies such as embryogenesis. The *C. elegans* completes its life cycle in three and a half days at 20 °C (Ref. 28). Therefore, its development is relatively fast (once the eggs are laid). Given this, hatching will take place in approximately 13 h (Ref. 11).

N2 wild-type *C. elegans* were grown in nematode growth media and fed with OP50 (*Escherichia coli*). Worms were synchronized, and embryos were obtained for the imaging experiments. Embryos from different developmental stages were mounted on a poly-L-lysine-Coated (Poly-L-lysine hydrobromide, Sigma Aldrich) thin coverslip (No. 0 thickness) with 10 μl of M9 buffer. The embryos where sandwiched between two thin glass coverslips, which were separated with 50-μm polystyrene microspheres (polymer microsphere suspension, Thermo Scientific). All this was done to avoid damaging and altering the embryos' original shape.[2] Samples were sealed with melted paraffin for sample stability and were imaged at constant room temperature (20 °C).

Control dishes containing nonirradiated *C. elegans* eggs were used to take into account other constraints that might prevent the embryos from developing. The survival rate for a total of 416 unexposed embryos was 89.2%.

2.3 *Two- and Three-Dimensional Time-Lapse Imaging*

Given that the maximum scanning speed of our galvanometric mirrors is ~300 lines/s, a single 2-D image of 500 × 500 pixels could be acquired in less than 2 s. For the purpose of this study and in order to improve the signal-to-noise ratio, one 2-D optical section is made of 10 averaged scans. (The whole process takes less than 20 s.)

To create a 3-D reconstruction of our specimen, a series of 2-D optical sections separated 1.3 μm apart were acquired. The choice of this parameter was based on the theoretical point spread function (PSF) axial resolution calculation (resulting value of 1.3 μm).[29] Given that the average sizes of the eggs are 60 × 30 × 30 μm, 24 planes are required to cover the whole specimen in the axial direction. In practice, 52 planes were taken into account for possible displacements of the sample. Thus, one full 3-D image was taken in approximately 15 min.

As no reference for the stress induced in the embryo or of sample deterioration at this specific wavelength is known, sample exposition and signal quality were adjusted according to the setup capabilities.

The images were volume rendered to allow for 3-D reconstruction employing ImageJ software. This procedure was repeated for different time points to enable a time-lapse 3-D reconstruction and further analysis.

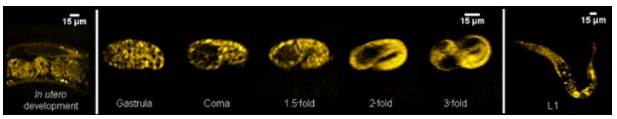

Fig. 2 THG images taken from several *C. elegans*, all at different developmental stages during the morphogenesis process. The THG signal is depicted in yellow. (Color online only.)

3 Results and Discussion

A total of 27 *C. elegans* embryos, at different developmental stages, were imaged. An emitted THG signal was observed in all the development stages as well as dynamic changes in its position and intensity along the different phases of the *C. elegans* wild-type embryos. Figure 2 depicts the *C. elegans* stages, starting from the cell division process inside the hermaphrodite, passing through the gastrula, coma, and multiple-fold stages (previous to the hatching process), and the L1 larva (after the hatching process).

At the early development stages, the emitted signal was generated from the individual cells (see Fig. 3). In later developmental stages occurring between the coma and the two-fold stages (see Fig. 4), the nerve and muscle cells start dif-

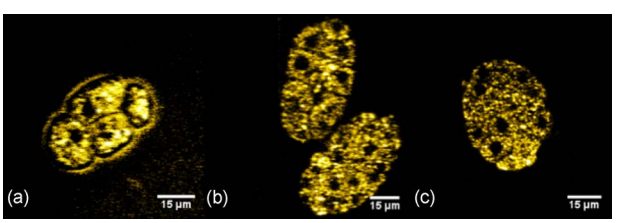

Fig. 3 THG images of several *C. elegans* embryos, all in the cell division stage. These images show identifiable dividing cells and nuclei (black circles inside delimited cells). The images depict (a) four-cell-stage egg; (b) and (c) multiple-cell-stage eggs. THG signal is depicted in yellow. (Color online only.)

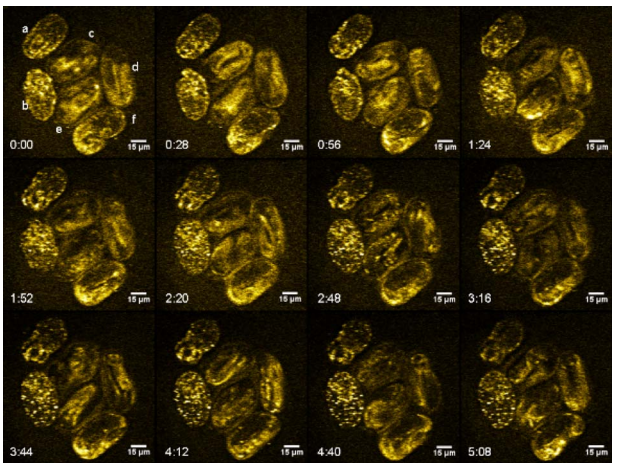

Fig. 4 THG images of six *C. elegans* embryos at different developmental stages. *a* and *b* are earlier developed (before ventral enclosure occurs); *c* to *f* are late developed (after ventral enclosure takes place). THG signal is depicted in yellow. Each frame is the average of 10 scans (taken in ~20 s). The sample was imaged during 5.08 h and the time between images is 28 min (See online Video 1 for a full animation of this sequence.) The shadow below the image is due to the M9 buffer–glass interface. (Color online only.)

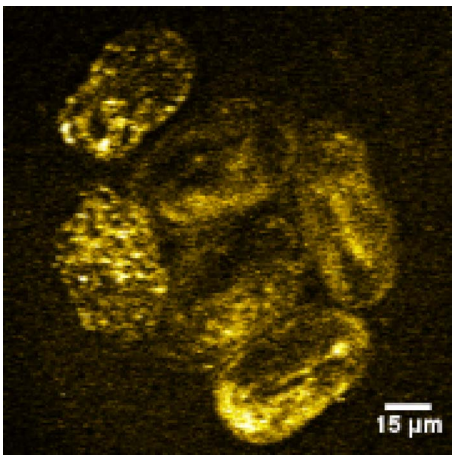

Video 1 THG animated time-lapse sequence in a 2-D reconstruction of six *C. elegans* embryos at different developmental stages. THG signal is depicted in yellow. The sample was imaged up to 5 h, and the time between images is 28 min. The shadow below the image is due to the M9 buffer–glass interface (QuickTime 2.4 MB). [URL: http://dx.doi.org/10.1117/1.3477535.1]

ferentiating. At this stage, the embryo begins to move inside the egg. In this case, the signal arose mainly from the outer layers of the embryo, becoming more restricted to tissue/structure. In what follows, all this will be further explained.

Figure 3 shows different embryos at the cell division stage (i.e., before gastrulation occurs). The emitted THG signal was observed in all the embryo cells (having the nuclei as a dark region due its homogeneous nature); thus, every cell can be outlined. During these stages, the cells contain lipid and carbohydrate depositions (i.e., vacuoles shown in bright yellow spots), which are internal storages that allow the embryos' development in the absence of external sources of energy. Due to these depositions, the embryos are able to complete the morphogenesis/embryogenesis process. These lipid depositions have already been suggested to give rise to the THG signal.[19,21,25,26]

In Fig. 4, we show a 2-D time-lapse recording (see Video 1 for the animated time-lapse sequence) of a group of embryos at different developmental stages. (The background of the image is due to the M9 buffer–glass interface.[30]) At the beginning of this time-lapse experiment, the acquired images allowed us to easily classify the embryos in two groups: the early stages, embryos labeled a and b, and the late stages (after ventral enclosure took place), embryos labeled c to f.

In this set of images, part of the *C. elegans* embryos' elongation process at the different developmental stages can be imaged. For the embryos in the early stage, this is particularly clear in embryo a, as it has been strategically positioned ventrally. For the more developed embryos, c to f (two- and threefold-stage embryos), this process can also be appreciated, although a detailed evolution cannot be imaged due to the intense movement, which is faster than our acquisition time (this will be further discussed later).

Moving forward in the developmental stages (starting from twofold stages, embryos c, d, e, and f in Fig. 4), the observed THG signal arose from a more superficial section of the embryo. This signal might be generated (in the twofold-stage embryo f) by tissues that could be body wall muscles or hypodermal cells (skin cells, ectoderm, etc.). For the more developed embryos c, d, and e (in threefold stage), such signal could possibly be attributed to the cuticle formation. The correct identification of the exact signal source is not within the scope of this work, which aims only to show the potential of the technique.

To further show the potential of this methodology, we proceed to obtain 4-D images of developing embryos. Figure 5 is a volume-rendered model of a *C. elegans* sample (rotated for a perspective view) taken at different times. In this figure, the 3-D time-lapse sequence enables us to follow the morphological evolution of five embryos (a and b earlier developed, c to e late developed).

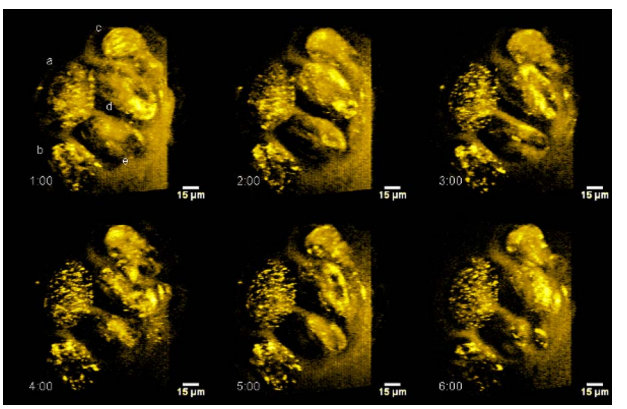

Fig. 5 3-D reconstruction of THG images (rotated for a perspective view) from *C. elegans* embryos at different developmental stages. The images were taken every 30 min during 6 h. (Shown times are $t=1$, 2, 3, 4, 5, and 6 h, respectively.) THG signal is depicted in yellow. (See online Video 2 for full 360-deg rotation of the initial image, $t=1$, followed by its temporal evolution.) The shadow below the image is due to the M9 buffer-glass interface. (Color online only.)

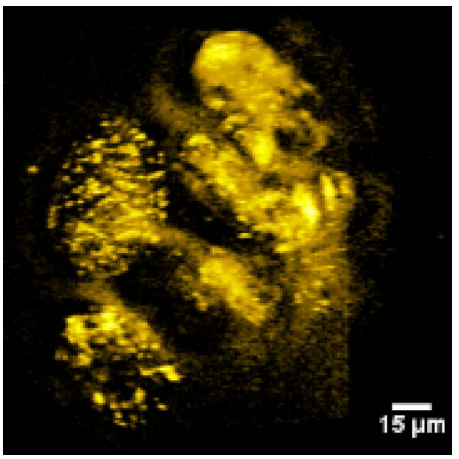

Video 2 THG animated time-lapse sequence in a four-dimensional reconstruction of *C. elegans* embryos at different developmental stages. The video depicts a 3-D image rotation. After the rotation finishes, the evolution of the embryos is shown in 4-D (time-lapse 3-D). The sample was imaged up to 6 h, and the time-lapse between 3-D images is 30 min. THG signal is depicted in yellow. The shadow below the image is due to the M9 buffer–glass interface (QuickTime 4.7 MB). [URL: http://dx.doi.org/10.1117/1.3477535.2]

In embryos a and b, the THG signal arose from the inner spots, which had a turning on and off (flashing) behavior during the different recorded time points. These strong blinking signals could be caused by the cell deaths, migrations, or fusions, or due to the loss of membrane integrity. All these processes occur particularly during the morphogenesis process. Additionally, as previously shown in Fig. 4, this 3-D model also aids us to easily identify the elongation process occurring in embryos c to e. It is worth mentioning that during two- and threefold stages, the cuticle synthesis begins and the embryos start to move rapidly (see Video 2 for full 360-deg rotation and evolution).

By close observation of Figs. 2–5, it is clear that the THG signal has the potential to provide us with a great amount of information occurring in the living *C. elegans* embryos at all the developmental stages, especially in the morphogenesis process. As stated earlier, using this imaging technique, one can clearly identify each developmental stage.

Here, it is important to mention that for interpreting the time-lapse images, care has to be taken in considering the speed limitations of our current setup, as explained in Sec. 2. In our case, our intention is to show the potential that this technique has for studying the distribution and evolution of the structures in this specimen. For detailed cell tracking studies, an optimized scan strategy should be employed. For instance, if only 24 stacks and single (not averaged) 2-D optical sections are used, it would be possible to perform 4-D recordings in a time period of 30 to 45 s per stack, according to Refs. 4 and 5. An optimized imaging system that takes into account dispersion for optimizing pulse duration at the sample plane of the microscope,[31] minimizing aberrations[26] (such as chromatic) and use of objectives optimized for such long wavelengths can be used for extracting more THG signal. If these considerations are taken into account, other scanning configurations could be used to speed up the scanning rates, such as acousto-optical deflectors[32] or a polygonal mirror.[33]

To further explore the induced effects of the 1550-nm wavelength, the survival rates of the embryos after long-term imaging exposure were studied. These rates were strongly dependent on the actual embryo development stage and the beginning of the time-lapse experiments. Thus, several long-term exposure trials (including the samples shown in this work) evaluating embryos' survival rates were performed. The samples were imaged for several hours and afterward left unexposed for another period of time to be able to hatch.

Based on our results, we were able to classify the specimen behavior in two main groups: embryos before twofold stage ($N=12$), and embryos after twofold stage ($N=15$). On one hand, the embryos before twofold had a survival rate of 41% (compared to our control sample). During the first hours, these embryos presented a normal development. Morphological processes such as gastrulation, cell migration, and fusion were recorded. However, in some cases, after long-term sample exposition, there was some slow down in development. A possible cause for this performance could be that during this stage, the embryo lacks differentiated tissue (i.e., hypodermic/ectodermic), making the differentiating cells more vulnerable to this kind of radiation.

On the other hand, and contrary to the less developed embryos, the twofold- and threefold-stage embryos had a survival rate of 73% (compared to our control sample). This was confirmed as the more developed embryos presented continuous muscular movement during the whole imaging process. In these experiments, the embryos presented a normal development without any detectable morphological defects (observable in the 2-D and 3-D volume-rendered images of Figs. 2–5, respectively). Moreover, as previously mentioned, even when threefold stage embryos were exposed up to 6 h, they were able to hatch normally. Based on these results, a possible cause for this performance could be that the development of structures like hypodermalectodermic tissue acts as a protection to infrared (IR) light exposure.

Although the hatching and the viability of the embryos and larvae cannot be considered an ideal indicator for the absence of possibly induced damage with this particular wavelength, our survival rate percentages, for the purpose of this work, were used as indicators of inflicted embryo damage. Moreover, a close anatomical observation of L1 larvae with DIC post-4-D imaging and the integrity of anatomical and behavioral characteristics of the larvae sustain our previous statement of reduced damage.

This work, in agreement with previous studies, has proven that THG modality at 1550 nm can be used to follow developmental processes of living unstained specimens (*Drosophila melanogaster* and Zebrafish)[19–22,25] for several hours. This is possible due to its optical noninvasive nature.

The application of this laser wavelength *in vivo*, and more importantly, its use for long-term 4-D imaging experiments (to record developing organisms such as *C. elegans* embryos) has enormous potential, not only because we are obtaining intrinsic signal from different structures inside the embryo (employing the sample interfaces as a contrast agent), but also because we are able to record embryogenesis/morphogenesis processes *in vivo*.

As previously demonstrated, embryogenesis/morphogenesis processes can take several hours. However, employing this particular wavelength, no apparent damage

was caused to the sample. These results were not expected, because it is known that IR wavelengths above 1500 nm are associated with increased water absorption in tissue and may lead to unwanted heating of biological specimens.[27] Additionally, due to the employed wavelength, the lateral and axial resolutions are reduced approximately by a factor of 2 when compared to that obtained with a Ti:Sapphire laser (at 800 nm and the same objective lens, NA=1.3).[27] Given this, one might think that this wavelength cannot be used for high-resolution imaging of living samples, nor for long-term imaging experiments. However, in our case, and in agreement with other works,[16–19,21,24–26,34] the laser used is able to produce an efficient THG signal from the sample using very low average powers. All this helps reduce the expected damage. In addition, the generated THG signal (516 nm) falls in the peak sensitivity region of most PMTs (i.e., Hamamatsu, H9305-04 peak sensitivity at 530 nm), allowing for an efficient signal collection. Another important and practical issue is that by using this wavelength, there is no requirement to use specialized collection optics (as is the case when conventional Ti:Sapphire lasers are used). Therefore, our results have demonstrated that this wavelength is suitable to perform 4-D imaging in living samples, e.g., *C. elegans,* and even in one of the most sensitive developmental stages of its life, such as embryogenesis.

One of the potential applications of this technique (either separately or in combination with the previously mentioned application) is cell tracking at early cell division stages. This is currently done with either DIC or fluorescence microscopy.[9] Consequently, tracking the cell division process is based on the image smoothness differences (i.e., the texture of the cytoplasm and spindles); therefore complex algorithms must be used. However, based on our results, the cell nucleus (at earlier stages), being a homogeneous structure, does not produce third-harmonic signal (in contrast with some surrounding structures). As a consequence, the presented images show that this structure is extremely clear and delimited (see Fig. 3).

All of the preceding indicates that the presented technique has the potential to be used as a tool for cell tracking when no fluorescent markers are available or desired for a particular reason. This type of information is relevant for cell lineage studies where these are tracked to determine which cells are precursors of different tissues. Importantly, this technique has the potential to provide enough information to easily identify the imaged structures without having to employ the previously mentioned complex image analysis algorithms to track the development of each structure.

Note that a frequency-doubled version of the same fiber laser source could be used for a multimodal microscopy approach, allowing the implementation of other techniques such as TPEF,[35] SHG,[14,15,19–22,25] etc. Adding these techniques will comprise an improved and supporting tool that would provide complementary information useful to investigate the source of the THG signal.

Last, the exact sources of the obtained THG signal in all development stages in the *C. elegans* embryos shown in this study still need to be investigated, and this is certainly a challenge in future work. Once the THG signal sources (in all the embryos' developmental stages and in the larvae) are identified, the requirement of using different reporters expressed in different cell types to track these types of processes could be bypassed. Then, the use of this technique, and this particular wavelength, could be used as a noninvasive technique to study different dynamic processes such as the development of certain cell/tissue precursors.

4 Conclusions

To the best of our knowledge, this is the first time that this wavelength is applied in THG imaging to perform morphogenesis/embryogenesis studies in living *C. elegans* embryos. We have demonstrated that using the 1550-nm wavelength, we are able to track *in vivo* morphological processes for several hours.

The fact that the THG emission is produced at 516 nm makes this wavelength very attractive for THG microscopy because many conventional detectors have their peak sensitivity within this range. Therefore, it enables the third-harmonic signal collection without having to employ specialized or UV-grade optics. In addition, the use of fiber-based laser systems will enable a simpler implementation on NLM, as they are compact, robust, and inexpensive.

THG microscopy provides the exact spatial localization of individual cells due to the 3-D sectioning capability. Importantly, its resolution enables the identification of individual cells and different structures present in the whole development cycle of the *C. elegans* worm. Therefore, it has the potential to be used to track the cells' positions and divisions during the morphological process. Given this, it could be possible to apply this methodology to perform cell lineage studies.

Certainly, this technique reduces the complexity of sample preparation required by other imaging techniques (fluorescence, confocal, and TPEF), as well as the interference with the specimen (genetic modification, fluorescent transgenes, dyes, etc.). Although the source of the THG signal has not been identified in all the developmental stages of the *C. elegans* embryo, we have shown that it is possible to outline a great potential use of this technique.

Acknowledgments

This work is supported by the Generalitat de Catalunya Grant No. 2009-SGR-159, a Spanish Government Grant No. TEC2009-09698, and EU Projects FAST DOT (FP7-ICT-2007-2, 224338) and STELUM (FP7-PEOPLE-2007-3-1-IAPP, 217997). This research has been partially supported by Fundació Cellex Barcelona. We would like to thank Johan Henriksson from the Karolinska Institutet and Jürgen Hench from the Institute of Pathology, University Hospital Basel, Schoenbeinstrasse, for their valuable input and discussions.

References

1. M. F. Portereiko and S. E. Mango, "Early morphogenesis of the *Caenorhabditis elegans* pharynx," *Dev. Biol.* **233**(2), 482–494 (2001).
2. J. Hench, J. Henriksson, M. Luppert, and T. R. Burglin, "Spatiotemporal reference model of *Caenorhabditis elegans* embryogenesis with cell contact maps," *Dev. Biol.* **333**(1), 1–13 (2009).
3. R. Schnabel, M. Bischoff, A. Hintze, A. K. Schulz, A. Hejnol, H. Meinhardt, and H. Hutter, "Global cell sorting in the *C. elegans* embryo defines a new mechanism for pattern formation," *Dev. Biol.* **294**(2), 418–431 (2006).
4. R. Schnabel, H. Hutter, D. Moerman, and H. Schnabel, "Assessing normal embryogenesis in *Caenorhabditis elegans* using a 4-D micro-

scope: variability of development and regional specification," *Dev. Biol.* **184**(2), 234–265 (1997).
5. C. Thomas, P. DeVries, J. Hardin, and J. White, "Four-dimensional imaging: computer visualization of 3-D movements in living specimens," *Science* **273**(5275), 603–607 (1996).
6. J. E. Sulston, E. Schierenberg, J. G. White, and J. N. Thomson, "The embryonic cell lineage of the nematode *Caenorhabditis elegans*," *Dev. Biol.* **100**(1), 64–119 (1983).
7. B. R. Masters, "Techniques that provide contrast," Chapter 5 in *Confocal Microscopy and Multiphoton Excitation Microscopy: The Genesis of Live Cell Imaging*, pp. 55–64, SPIE Press, Bellingham, WA (2006).
8. M. Oheim, D. J. Michael, M. Geisbauer, D. Madsen, and R. H. Chow, "Principles of two-photon excitation fluorescence microscopy and other nonlinear imaging approaches," *Adv. Drug Delivery Rev.* **58**(7), 788–808 (2006).
9. S. Hamahashi and S. Onami, "Objective measurement of spindle orientation in early *Caenorhabditis elegans* embryo," *Genome Informatics* **16**(2), 86–93 (2005).
10. J. T. Yasuda, H. Bannai, S. Onami, S. Miyano, and H. Kitano, "Toward automatic construction of cell-lineage of *C. elegans* from Nomarski DIC microscope images," *Genome Informatics* **10**, 144–165 (1999).
11. Z. Bao, J. I. Murray, T. Boyle, S. L. Ooi, M. J. Sandel, and R. H. Waterson, "Automated cell linage tracing in *Caenorhabditis elegans*," *PNAS* **103**(8), 2707–2712 (2006).
12. S. Hamahashi, S. Onami, and H. Kitano, "Detection of nuclei in 4-D Nomarski DIC microscope images of early *Caenorhabditis elegans* embryos using local image entropy and object tracking," *BMC Bioinf.* **6**(125), 1–15 (2005).
13. W. A. Mohler and J. G. White, "Multiphoton laser scanning microscopy for four-dimensional analysis of *Caenorhabditis elegans* embryonic development," *Opt. Express* **3**(9), 325–331 (1998).
14. S. Psilodimitrakopoulos, D. Artigas, G. Soria, I. Amat-Roldán, A. M. Planas, and P. Loza-Álvarez, "Quantitative discrimination between endogenous SHG sources in mammalian tissue, based on their polarization response," *Opt. Express* **17**(12), 10168–10176 (2009).
15. S. Psilodimitrakopoulos, V. Petegnief, G. Soria, I. Amat-Roldan, D. Artigas, A. M. Planas, and P. Loza-Alvarez, "Estimation of the effective orientation of the SHG source in cortical neurons," *Opt. Express* **17**(16), 14418–14425 (2009).
16. E. J. Gualda, G. Filippidis, M. Mari, G. Voglis, M. Vlachos, C. Fotakis, and N. Tavernarakis, "*In vivo* imaging of neurodegeneration in *Caenorhabditis elegans* by third-harmonic generation microscopy," *J. Microscop. Oxford* **232**(2), 270–275 (2008).
17. R. Aviles-Espinosa, G. J. Tserevelakis, S. I. C. O. Santos, G. Filippidis, A. J. Krmpot, M. Vlachos, N. Tavernarakis, A. Brodschelm, W. Kaenders, D. Artigas, and P. Loza-Alvarez, "Cell division stage in *C. elegans* imaged using third-harmonic generation microscopy," in *Proc. Biomedical Optics*, Optical Society of America, Wasington, D.C., p. BTuD78 (2010).
18. G. J. Tserevelakis, G. Filippidis, A. J. Krmpot, M. Vlachos, C. Fotakis, and N. Tavernarakis, "Imaging *Caenorhabditis elegans* embryogenesis by third-harmonic generation microscopy," *Micron* **41**(5), 444–447 (2010).
19. W. Supatto, D. Débarre, B. Moulia, E. Brouzés, J. L. Martin, E. Farge, and E. Beaurepaire, "*In vivo* modulation of morphogenetic movements in Drosophila embryos with femtosecond laser pulses," *PNAS* **102**(4), 1047–1052 (2005).
20. S. W. Chu, S. Y. Chen, T. H. Tsai, and T. M. Liu, "*In vivo* developmental biology study using noninvasive multi-harmonic generation microscopy," *Opt. Express* **11**(23), 3093–3099 (2003).
21. D. Debarre, W. Supatto, E. Farge, B. Moulia, M. C. Schanne-Klein, and E. Beaurepaire, "Velocimetric third-harmonic generation microscopy: micrometer-scale quantification of morphogenetic movements in unstained embryos," *Opt. Lett.* **29**(104), 2881–2883 (2004).
22. C. K. Sun, S. W. Chu, S. Y. Chen, T. H. Tsai, T. M. Liu, C. Y. Lin, and H. J. Tsai, "Higher harmonic generation microscopy for developmental biology," *J. Struct. Biol.* **147**(1), 19–30 (2004).
23. L. Moreaux, O. Sandre, M. Blanchard-Desce, and J. Mertz, "Membrane imaging by simultaneous second-harmonic generation and two-photon microscopy," *Opt. Lett.* **25**(5), 678 (2000).
24. A. C. Millard, P. W. Wiseman, D. N. Fittinghoff, K. R. Wilson, J. A. Squier, and M. Muller, "Third-harmonic generation microscopy by use of a compact, femtosecond fiber laser source," *Appl. Opt.* **38**(36), 7393–7397 (1999).
25. D. Debarre, W. Supatto, A. M. Pena, A. Fabre, T. Tordjmann, L. Combettes, M. C. Schanne-Klein, and E. Beaurepaire, "Imaging lipid bodies in cells and tissues using third-harmonic generation microscopy," *Nat. Methods* **3**(1), 47–53 (2006).
26. A. Jesacher, A. Thayil, K. Grieve, D. Debarre, T. Watanabe, T. Wilson, S. Srinivas, and M. J. Booth, "Adaptive harmonic generation microscopy of mammalian embryos," *Opt. Lett.* **34**(20), 3154–3156 (2009).
27. D. Yelin, D. Oron, E. Korkotian, M. Segal, and Y. Silberberg, "Third-harmonic microscopy with a titanium-sapphire laser," *Appl. Phys. B* **74**(9), 97–101 (2002).
28. I. A. Hope, "The genome project and sequence homology to other species," Chapter 2 in *C. Elegans; A Practical Approach*, pp. 17–33, Oxford University Press, Oxford, New York (1999).
29. W. R. Zipfel, R. M. Williams, and W. W. Webb, "Nonlinear magic: multiphoton microscopy in the biosciences," *Nat. Biotechnol.* **21**(11), 1369–1377 (2003).
30. P. Török and F. Kao, "Parametric nonlinear optical techniques in microscopy," Chapter 8 in *Optical Imaging and Microscopy*, pp. 197–214, Springer Series, Berlin–Heidelberg (2003).
31. A. K. N. Thayil, E. J. Gualda, S. Psilodimitrakopoulos, I. G. Cormack, I. Amat-Roldán, M. Mathew, D. Artigas, and P. Loza-Alvarez, "Starch-based backward SHG for *in situ* MEFISTO pulse characterization in multiphoton microscopy," *J. Microsc.* **230**(1), 70–75 (2008).
32. Y. Kremer, J.-F. Léger, R. Lapole, N. Honnorat, Y. Candela, S. Dieudonné, and L. Bourdieu, "A spatio-temporally compensated acousto-optic scanner for two-photon microscopy providing large field of view," *Opt. Express* **16**(14), 10066–10076 (2008).
33. K. H. Kim, C. Buehler, and P. T. C. So, "High-speed, two-photon scanning microscope," *Appl. Opt.* **38**(28), 6004–6009 (1999).
34. G. Filippidis, E. J. Gualda, M. Mari, K. Troulinaki, C. Fotakis, and N. Tavernarakis, "*In vivo* imaging of cell morphology and cellular processes in *Caenorhabditis elegans*, using nonlinear phenomena," *Micron* **40**(8), 876–880 (2009).
35. M. Mathew, S. I. C. O. Santos, D. Zalvidea, and P. Loza-Alvarez, "Multimodal optical workstation for simultaneous linear, nonlinear microscopy and nanomanipulation: upgrading a commercial confocal inverted microscope," *Rev. Sci. Instrum.* **80**(7), 073701 (2009).